

# Evidence for Conductive $\text{Cl}^-$ Pathways across the Cell Membranes of the Thin Ascending Limb of Henle's Loop

Koji Yoshitomi, Yoshiaki Kondo, and Masashi Imai

Department of Pharmacology, National Cardiovascular Center, Research Institute, Osaka 565, Japan

## Abstract

To examine whether  $\text{Cl}^-$  is transported via transcellular pathways in the thin ascending limb of Henle's loop (TAL), conventional microelectrode technique was applied in isolated TAL segments of hamsters perfused *in vitro*. The average basolateral membrane voltage ( $V_B$ ) was  $-24.5 \pm 1.5$  mV ( $n = 18$ ). Ouabain ( $10^{-4}$  M) had no effect on  $V_B$ . Sudden reduction of basolateral  $\text{Cl}^-$  concentration from 165 to 5 mmol/liter caused a large depolarizing spike ( $+49.1 \pm 2.7$  mV,  $n = 18$ ), while the transepithelial potential ( $V_T$ ) showed lumen positive deflection by  $33.4 \pm 1.2$  mV, which indicates that a large  $\text{Cl}^-$  conductance exists in the basolateral membrane. Reduction of luminal  $\text{Cl}^-$  concentration caused sustained depolarization of luminal cell membrane from  $+24.5 \pm 2.1$  to  $-9.7 \pm 3.4$  mV ( $n = 6$ ), which indicates that there is also a  $\text{Cl}^-$  conductance in the luminal membrane. Since we have previously shown that acidification of ambient solution suppresses the transmural  $\text{Cl}^-$  permeability, we tested whether acid pH also inhibits the  $\text{Cl}^-$  conductance of the basolateral membrane. When pH of the bathing fluid was lowered to 5.8, the depolarizing spike of  $V_B$  and the change of  $V_T$  upon sudden reduction of basolateral  $\text{Cl}^-$  were almost completely abolished. From these results we conclude: (a) both the luminal and the basolateral membrane of hamster TAL segments have  $\text{Cl}^-$  conductances, and (b)  $\text{Cl}^-$  transport in the TAL takes place, at least in part, via a transcellular route when a transepithelial  $\text{Cl}^-$  gradient is present.

## Introduction

Although NaCl transport across the thin ascending limb of Henle's loop (TAL)<sup>1</sup> is assumed to play an integral part in the generation of renal medullary osmotic gradient, the mechanism of NaCl transport across this segment is unknown (1). The *in vitro* microperfusion studies have revealed that the TAL is characterized by a high permeability to NaCl, a moderate permeability to urea, and a low permeability to water (2–4). Imai and Kokko (5) have proposed that  $\text{Cl}^-$  is transported across the TAL by facilitated diffusion based on the

following observations: (a) the unidirectional  $\text{Cl}^-$  flux exhibited saturation kinetics, (b) the  $\text{Cl}^-$  flux was competitively inhibited by  $\text{Br}^-$ , and (c) the flux ratios for  $\text{Cl}^-$  deviated from the line predicted from simple passive diffusion.

Recently, we (5) demonstrated that in hamster TAL the  $\text{Cl}^-$  transport was inhibited by anion transport inhibitors including stilbene disulfonates, phloretin, and furosemide. We further demonstrated that the  $\text{Cl}^-$  transport across the TAL was not coupled with  $\text{Na}^+$ ,  $\text{K}^+$ , or  $\text{HCO}_3^-$  (5). Based on these observations we proposed that the  $\text{Cl}^-$  transport across the TAL is mediated by electrodiffusion. We also reported that the  $\text{Cl}^-$  conductance across the hamster TAL is regulated by pH (6) as well as by  $\text{Ca}^{2+}$  (7).

Although it is reasonable to assume that such a special transport process for  $\text{Cl}^-$  may be located in cell membranes and that a significant portion of  $\text{Cl}^-$  is transported via a transcellular route, no direct evidence is available to support this notion. To resolve this problem, it is essential to impale cells with microelectrodes, an extremely difficult task which, to our knowledge, no one has ever tried thus far. We have recently succeeded in impaling cells of the hamster TAL perfused *in vitro* with a microelectrode. The main purpose of this paper is to report the evidence that indicates that the cell membranes of the TAL have a large  $\text{Cl}^-$  conductance which is modulated by ambient pH.

## Methods

The *in vitro* microperfusion of isolated renal tubule was used according to the method of Burg et al. (8) with slight modifications as reported previously (9). Either male or female golden hamsters (50–80 g) were used. They were maintained on regular laboratory chow and allowed free access to tap water. After the animals had been anesthetized with pentobarbital (50 mg/kg, body weight, *i.p.*), both kidneys were removed. Slices of coronary section of 1–2-mm thickness were made and transferred to a cooled dish (4–6°C) containing an artificial solution. Segments of the TAL were dissected by using sharpened forceps under a stereomicroscope. The criteria of identifying TAL have already been reported (2). The segment was identified by confirming the abrupt transition to the thick ascending limb at the border between the inner and the outer medulla. Tubules were dissected at the transitional portion from the thin to thick limb. The isolated segments were hooked up by the thick portion to the holding pipette for perfusion. *In vitro* perfusion system was modified in our laboratory for the use of intracellular microelectrodes (9). Since the details of the technique have been published previously, they will be presented here only in brief. The tubule was suspended between two pipettes, and routinely cannulated with a double-barrelled perfusion pipette (theta-borosilicate glass, 1402401; Hilgenberg, Malsfeld FRG). The transepithelial voltage ( $V_T$ ) was measured through one barrel of the perfusion pipette, which was connected to one channel of a dual electrometer (FD 223; WP-Instruments, New Haven, CT) with a 1-M KCl agar bridge and a calomel half cell. Exchange of luminal fluid was performed by using the other barrel of the perfusion pipette. The time required for fluid exchange was < 1 s. Luminal perfusion rate exceeded 10 nl/min in all studies. We used a

Address all correspondence to Dr. Koji Yoshitomi, Department of Pharmacology, National Cardiovascular Center, Research Institute, 5-7-1 Fujishirodai, Suita, Osaka 565, Japan.

Received for publication 27 May 1987 and in revised form 4 June 1988.

1. Abbreviations used in this paper: TAL, thin ascending limb of Henle's loop;  $V_A$ , apical membrane voltage;  $V_B$ , basolateral membrane voltage;  $V_T$ , transepithelial voltage.

J. Clin. Invest.

© The American Society for Clinical Investigation, Inc.

0021-9738/88/09/0866/06 \$2.00

Volume 82, September 1988, 866–871

rapid bath flow system that allowed us to exchange the entire bath volume (100  $\mu$ l) within 1 s (9). A flowing boundary 1-M KCl bridge connected to a calomel half cell was placed at the outflow of the bath and served as a system ground.

The basolateral membrane voltage ( $V_B$ ) was measured with conventional microelectrodes, which were pulled from borosilicate glass tubing of 1.5-mm outside diameter and 0.87-mm inside diameter (1403521; Hilgenberg) on a vertical puller (PE-2; Narishige, Tokyo, Japan). They were filled with 1 M Na-formate and 5 mM KCl solution and had resistances of 150–200 M $\Omega$  and negligible tip potentials ( $< 5$  mV). They were fixed to a microelectrode holder containing a Ag/AgCl-pellet, and connected to a high input impedance electrometer (FD 223). To impale tubular cells, a microelectrode was positioned against the basolateral membrane with a hydraulic micromanipulator (MO-102N; Narishige), which was mounted on another micromanipulator (MN-1; Narishige) that was fixed to the stage of a microscope (IMT-2; Olympus, Tokyo, Japan). The microelectrode was advanced into the cell by tapping the air-cushioned table or the body of the microscope. All voltages ( $V_B$ ,  $V_T$ ) were recorded on a multipen recorder (R-306; Rikadenki, Tokyo, Japan).

The criteria that we set for acceptability of an intracellular voltage recording were (a) an abrupt change in the potential difference read by the microelectrode, (b) stability of the basolateral membrane potential for at least 20 s, and (c) return of the membrane potential to the baseline upon withdrawal of the microelectrode. In all experiments, we checked for proper intracellular positioning of the microelectrode by testing for the fast voltage deflection which occurs in response to abruptly reducing the bath  $\text{Cl}^-$  concentration.

The standard artificial solution used in this study contained in millimoles per liter  $\text{Na}^+$ , 160.9;  $\text{K}^+$ , 5.0;  $\text{Cl}^-$ , 165;  $\text{Ca}^{2+}$ , 1.5;  $\text{Mg}^{2+}$ , 1.0; acetate, 2.5; phosphate, 0.5; Hepes, 5.0; 2-*N*-morpholinoethane-sulfonic acid, 5.0; and urea, 270. Total osmolality was 620 mosmol/kg  $\text{H}_2\text{O}$ . pH was adjusted to 7.40 with Tris or NaOH when it was not otherwise specified. When the effect of an abrupt decrease in  $\text{Cl}^-$  concentration of the bathing fluid was examined, 160 mmol NaCl was replaced by equimolar Na gluconate (5 mmol/liter  $\text{Cl}^-$  solution).

All the values were expressed as the means  $\pm$  SEM. Comparison between two groups was made using either paired or nonpaired Student *t* test when appropriate. *P* values  $< 0.05$  were considered to be significant.

## Results

**Cell membrane voltage.** Since this was the first trial of recording the cell membrane voltage in the TAL, we had to take special care whether the tip of the microelectrode was inside a cell. Initially, we used the increase in the input resistance of the microelectrode as an indicator of a successful intracellular impalement. However, after preliminary experiments had shown the existence of a  $\text{Cl}^-$  conductance in the basolateral membrane (see below), we employed the maneuver of basolateral  $\text{Cl}^-$  reduction as a tool to verify proper intracellular punctures.

In most cases, the potential time course after the impalement of a cell with a microelectrode was characterized by an initial spike and a subsequent decay of the potential toward the baseline level. Of more than a 1,000 tries to impale the cells, only 18 punctures were accepted as successful. In these recordings, after the initial abrupt change upon impalement, the voltage had remained stable for several minutes.  $V_B$  of TAL ranged from  $-14.0$  to  $-40.0$  mV with a mean of  $-24.5 \pm 1.5$  mV ( $n = 18$ ), while the  $V_T$  was virtually zero. The frequency distribution of  $V_B$  was nearly Gaussian (Fig. 1). To test whether the Na-K pump contributes to the intracellular voltage, we looked for an effect of ouabain ( $10^{-5}$  mol/liter), which was added to

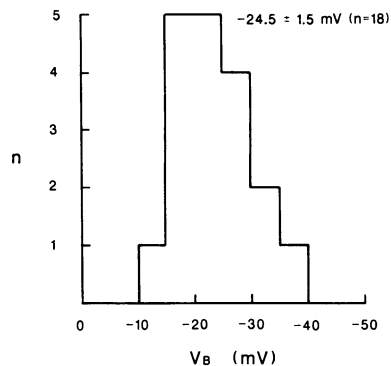


Figure 1. Frequency distribution of  $V_B$  of hamster TAL.

the bathing fluid, on  $V_B$  ( $n = 5$ ). However, in these experiments  $V_B$ , which was  $-20.4 \pm 1.7$  mV in the control state, did not change after ouabain ( $-20.2 \pm 1.7$  mV).

**Basolateral  $\text{Cl}^-$  conductance.** In searching for a  $\text{Cl}^-$  conductance in the basolateral cell membrane we studied the effect on  $V_B$  of abruptly reducing the bath  $\text{Cl}^-$  concentration. Fig. 2 shows a representative tracing of a cell puncture, where a concentration step of  $\text{Cl}^-$  from 165 to 5 mmol/liter was imposed. As can be seen in this figure, a large depolarizing spike was observed upon the sudden reduction of basolateral  $\text{Cl}^-$  concentration, which was followed by a gradual repolarization. Hyperpolarization was observed upon restoration of  $\text{Cl}^-$  concentration.

If we assume that the cell membranes are impermeable for gluconate, we can interpret the large depolarizing spike as indicating an efflux of negative charge ( $\text{Cl}^-$ ) from the cell, which suggests the existence of a  $\text{Cl}^-$  conductance in the basolateral membrane. The results of 18 experiments are summarized in Table I. The mean value of the depolarizing spike was  $+49.1$  mV. Simultaneously with the spike,  $V_T$  changed to 33.4 mV lumen positive, which indicates the  $\text{Cl}^-$  permselectivity of TAL segment.

In the preliminary experiments, when applying  $\text{Na}^+$ -free or  $\text{K}^+$ -rich (50 mM) solution either to the lumen or to the bath,

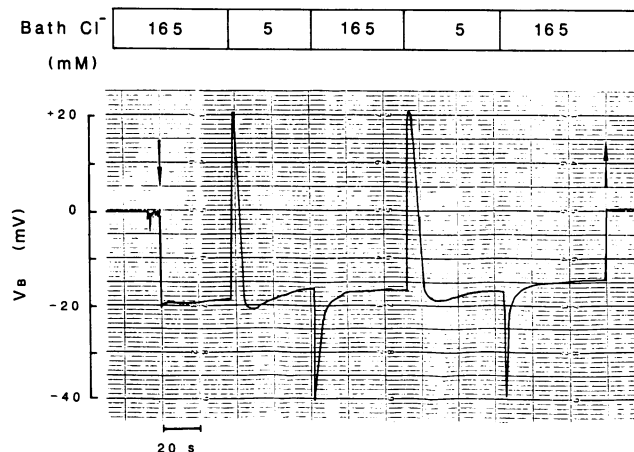


Figure 2. Effect of sudden reduction of basolateral  $\text{Cl}^-$  concentration from 165 to 5 mmol/liter on  $V_B$ . Arrows, cell puncture and withdrawal of microelectrode.

Table I. Effect of Abrupt Reduction of  $\text{Cl}^-$  Concentration in the Bath From 165 to 5 meq/liter on  $V_T$  and  $V_B$

Voltage	Control	$\text{Cl}^-$ gradient (bath)
<i>mV</i>		
$V_T$	$0 \pm 0.1$	$+33.4 \pm 1.2$
$\Delta V_T$		$+33.4 \pm 1.2$ ( $P < 0.001$ )
$V_B$	$-24.5 \pm 1.5$	$+24.6 \pm 3.2^*$
$\Delta V_B$		$+49.1 \pm 2.7$ ( $P < 0.001$ )

Results of 18 experiments are shown.

$\Delta$ , Change after imposing a  $\text{Cl}^-$  concentration gradient.

\* The peak value upon sudden reduction of basolateral  $\text{Cl}^-$  concentration.

we did not find any evidence for either a  $\text{K}^+$  conductance or an  $\text{Na}^+$  conductance in either of the cell membranes.

**Luminal  $\text{Cl}^-$  conductance.** The  $V_T$  of the TAL was virtually zero ( $0 \pm 0$  mV), when the perfusate composition was identical on both surfaces of the epithelium. However, a diffusion voltage was generated when a  $\text{Cl}^-$  gradient was imposed. Although, in accord with a previous report (4), we confirmed that the diffusion voltage was almost symmetrical when the  $\text{Cl}^-$  gradient was imposed from lumen to bath or vice versa (data not shown). This does not necessarily mean the  $\text{Cl}^-$  conductance is localized exclusively in the paracellular pathway. The existence of a  $\text{Cl}^-$  conductance in the apical and basolateral membranes in series could also account for the symmetrical diffusion voltage. To confirm that there is also a  $\text{Cl}^-$  conductance in the luminal membrane, we tested the effect of a sudden reduction of luminal  $\text{Cl}^-$  concentration on luminal membrane voltage ( $V_A$ ).  $V_A$  was defined as  $V_T - V_B$ . A representative study is shown in Fig. 3, and a summary of six experiments is shown in Table II. By this maneuver,  $V_T$  changed from zero to  $-31.8$  mV, whereas  $V_B$  changed little, from  $-24.5$  to  $-22.2$  mV, without exhibiting a transient spike. The calculated  $V_A$  was

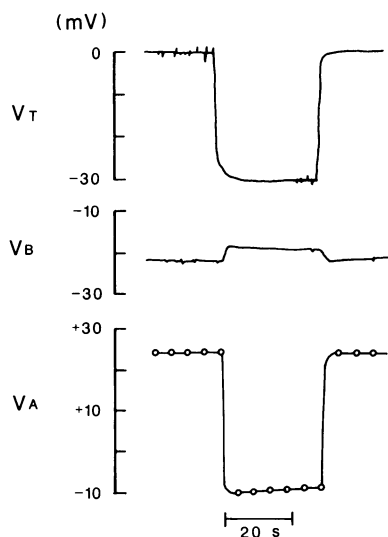


Figure 3. Effect of luminal  $\text{Cl}^-$  reduction from 165 to 5 mmol/liter on  $V_T$ ,  $V_B$ , and  $V_A$ .  $V_A$  values were calculated as  $V_T - V_B$  and were plotted at intervals of 5 s.

Table II. Effect of Abrupt Reduction of  $\text{Cl}^-$  Concentration in the Lumen From 165 to 5 meq/liter on  $V_T$ ,  $V_B$ , and  $V_A$

Voltage	Control	$\text{Cl}^-$ gradient (lumen)
<i>mV</i>		
$V_T$	$0 \pm 0$	$-31.8 \pm 2.3$
$\Delta V_T$		$-31.8 \pm 2.2$ ( $P < 0.001$ )
$V_B$	$-24.5 \pm 2.1$	$-22.2 \pm 2.2$
$\Delta V_B$		$+2.3 \pm 0.4$ ( $P < 0.01$ )
$V_A$	$+24.5 \pm 2.1$	$-9.7 \pm 3.4$
$\Delta V_A$		$-34.2 \pm 1.9$ ( $P < 0.001$ )

Results of six experiments are shown.  $P < 0.001$  as compared with zero.

24.5 mV (cell inside was supposed to be zero potential) in control state and  $-9.7$  mV after luminal  $\text{Cl}^-$  reduction. The average value of depolarization of  $V_A$  was 34.2 mV, indicating that there is an apparent  $\text{Cl}^-$  conductance in the luminal cell membrane as well.

**Effect of low pH on basolateral  $\text{Cl}^-$  conductance.** A recent study from our laboratory showed that  $\text{Cl}^-$  transport across the TAL was inhibited by ambient acid pH (6). To confirm whether acid pH affects the transcellular  $\text{Cl}^-$  movement via the previously described  $\text{Cl}^-$  conductance, we examined the effect of acidification of the bathing fluid on the depolarizing spike induced by sudden reduction of  $\text{Cl}^-$  concentration. A representative tracing is shown in Fig. 4. After confirming that a sudden reduction of basolateral  $\text{Cl}^-$  concentration induced a large depolarizing spike of  $V_B$ , the bathing solution was made acid (pH 5.8). Although the basal level of  $V_B$  was unaffected by this procedure, the subsequent change of  $\text{Cl}^-$  concentration markedly reduced the magnitude of the depolarizing spike. The response was restored after the bathing pH was normalized. Similar observations were made in seven experiments. The magnitude of the depolarizing spike of  $V_B$  decreased from

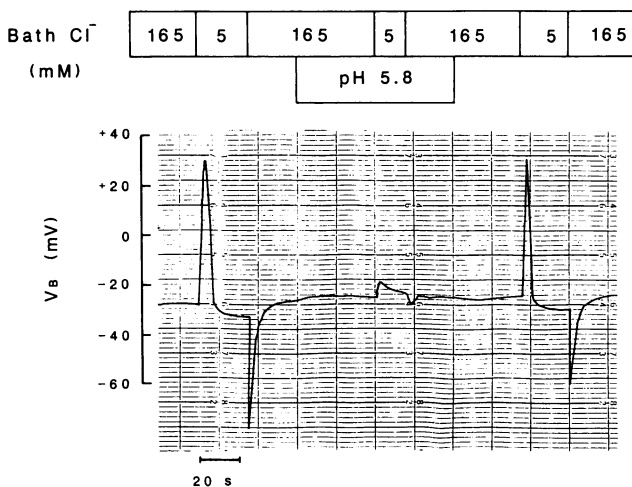


Figure 4. Effect of low pH on the response of  $V_B$  to reduction of bath  $\text{Cl}^-$  concentration. Note that the depolarizing spike of  $V_B$  was abolished under low pH.

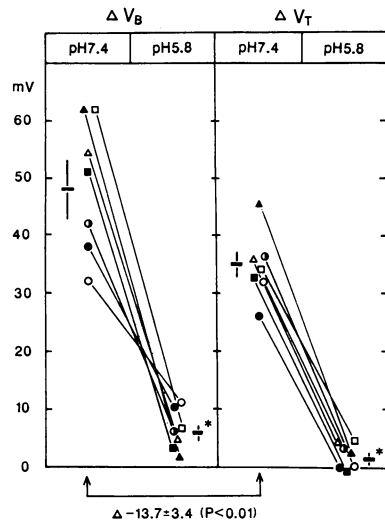


Figure 5. Effect of low pH on the responses of  $\Delta V_B$  and  $\Delta V_T$  to bath  $\text{Cl}^-$  reduction. Bars, mean values and SEM. The data indicated by same symbols are derived from the same preparations. \* $P < 0.001$  with the values of pH 7.4.

$48.7 \pm 4.4$  to  $6.0 \pm 1.3$  mV ( $P < 0.001$ ) because of the acidification of the bathing fluid. The simultaneous response of  $V_T$  to basolateral  $\text{Cl}^-$  reduction also decreased from  $35.0 \pm 2.3$  to  $1.3 \pm 0.7$  mV ( $P < 0.001$ ) because of this procedure (Fig. 5).

## Discussion

In the present study, we succeeded for the first time to impale the epithelial cells of the TAL with conventional microelectrodes in order to obtain the transcellular voltage profile. Furthermore, by investigating cell membrane potential changes in response to ambient ion concentration, we obtained direct evidence for the existence of  $\text{Cl}^-$  conductances in both the luminal and basolateral membranes. Since we have carefully adhered to the previously mentioned impalement criteria, we are convinced that our techniques are appropriate, and hence that our data are meaningful. There is no doubt, at least, with regard to the proper intracellular localization of the electrode. This is clearly documented by the recorded potential transients (in response to reduction of bath  $\text{Cl}^-$  concentration), which were clearly distinct from the response of the  $V_T$ . Less clear may be the absolute value of  $V_B$ .

We found that  $V_B$  was  $-24.5$  mV under control conditions. In contrast to most epithelia, the observed  $V_B$  was insensitive to ouabain. This, however, is in accord with our previous observations that no net solute flux was detectable (2) and that in the absence of external passive driving forces  $\text{Cl}^-$  transport was not affected by ouabain (5). Although the presence of a small quantity of  $\text{Na}^+$ - $\text{K}^+$ -ATPase was demonstrated by using a monoclonal antibody (10), our data suggest that the  $\text{Na}^+$ - $\text{K}^+$  pump does not contribute in a major way to the generation of the basal membrane voltage. Previous studies (11, 12) even failed to demonstrate  $\text{Na}^+$ - $\text{K}^+$ -ATPase activity in the TAL when using a microchemical technique. Altogether, at the present time, we do not know the source of the membrane voltage. Donnan's equilibrium potential or other active rheogenic pumps, such as  $\text{H}^+$ -ATPase and  $\text{Ca}^{2+}$ -ATPase, might be responsible for it. The basolateral membrane has a large  $\text{Cl}^-$  conductance which constitutes a major part of the conductive pathway across this membrane.

By using the Goldman-Hodgkin-Katz equation and assuming that intracellular ion activities were unchanged at the peak time of the voltage deflection, the change in  $V_B$  ( $\Delta V_B$ ) upon sudden reduction of basolateral  $\text{Cl}^-$  concentration can be expressed as follows:

$$\Delta V_B = \frac{RT}{F} \ln \frac{P_{\text{Na}}(a_{\text{Na}})_C + P_{\text{K}}(a_{\text{K}})_C + P_{\text{Cl}}(a_{\text{Cl}})_{B'}}{P_{\text{Na}}(a_{\text{Na}})_C + P_{\text{K}}(a_{\text{K}})_C + P_{\text{Cl}}(a_{\text{Cl}})_B} \quad (1)$$

where  $R$ ,  $T$ , and  $F$  are gas constant, absolute temperature, and Faraday constant, respectively,  $P$  is permeability for the ion shown by subscript,  $a$  is the ion activity, subscripts  $B$  and  $B'$  denote bathing fluid before and after  $\text{Cl}^-$  reduction, respectively, and subscript  $C$  indicates intracellular fluid. If this membrane was purely permeable for  $\text{Cl}^-$ , a reduction of bath  $\text{Cl}^-$  concentration from 165 to 5 mmol/liter should have caused a 93-mV depolarization. However, the observed depolarization in response to such a  $\text{Cl}^-$  step was 49.1 mV. Several explanations can be offered for the discrepancy between the Nernstian slope and the observed response of  $V_B$  upon reduction of bath  $\text{Cl}^-$  concentration. First, reduced Nernstian slope means that we cannot neglect permeabilities for  $\text{Na}^+$  and/or  $\text{K}^+$  in Eq. 1, although we could not detect sizable conductances of  $\text{Na}^+$  or  $\text{K}^+$  at least in the experimental condition tested. Second, the liquid junction potential generated by bath  $\text{Cl}^-$  reduction might be responsible for the reduced Nernstian slope. Calculated value of junction potential between 165 and 5 mmol/liter  $\text{Cl}^-$  solution is 11 mV (13), which also causes an underestimation of  $\text{Cl}^-$  conductance. However, this possibility is less likely because we are using a flowing boundary 1-M KCl bridge and hence liquid junction potential would be minimized. Third, the circular current created by the change of electromotive force may flow from one to the other cell membrane in the presence of a high paracellular shunt. This would also cause a diminution of the change of  $V_B$  in response to bath  $\text{Cl}^-$  reduction. Finally, it is possible that the exchange of bath fluid, even though it took only 1 s, was not rapid enough to achieve the full size of the depolarizing spike and that ideally the true response of  $V_B$  could have been even closer to the theoretical value. The same is true for the luminal membrane, in which the  $\text{Cl}^-$  conductance also exists, although the magnitude of the  $\text{Cl}^-$  conductance seems to be less than that of the basolateral membrane ( $+34.2$  mV vs.  $+49.1$  mV).

In previous studies (5–7), we have suggested that  $\text{Cl}^-$  is transported, at least in part, through the cell membranes. This was based on the observation that either selective intracellular acidification with *o*-nitrophenyl acetate (6) or selective intracellular  $\text{Ca}^{2+}$  chelating with quin-2 AM inhibited the  $\text{Cl}^-$  conductance (7). The present study provides further, more direct, evidence in support of this view. Because of the morphology of the tight junction of the TAL (14–16), it is reasonable to assume that this segment has leaky tight junctions. Therefore, we wanted to know which proportion of the total  $\text{Cl}^-$  conductance can be accounted for by the paracellular pathway. By using the changes of  $V_B$  and  $V_T$  upon sudden reduction of basolateral  $\text{Cl}^-$  concentration, we can assess the relative contribution of the transcellular or paracellular component to the net  $\text{Cl}^-$  transport. For this purpose, we used the equivalent circuit analysis of single cell layered epithelia (17). It should be mentioned that this treatment does not deal with the changes in membrane resistances which may be expected to occur in ion

substitution experiments. Although our experimental condition is within the linear range of macroconductance measured by transepithelial voltage deflection in response to varying steps of  $\text{Cl}^-$  concentration (data not shown), it might be that single channel conductance is dependent on  $\text{Cl}^-$  concentration and that open and closed kinetics are affected by voltage (18). Hence, it is possible that the conductance of the basolateral membrane might behave in a nonlinear fashion. However, since the microconductance measurement is not feasible at present, we assume that all resistances are constant during bath  $\text{Cl}^-$  reduction in the following treatment. The simplest equivalent circuit for the TAL segment consists of three transmural barriers: the luminal membrane, the basolateral membrane, and the paracellular shunt pathway. At each of the barriers, a single equivalent electromotive force ( $E_A$ ,  $E_B$ , and  $E_S$ ) and an equivalent electrical resistance ( $R_A$ ,  $R_B$ , and  $R_S$ ) represent the dissipative ionic processes. Each of the potential differences ( $V_B$ , and  $V_T$ ) is a function of all the electromotive forces and resistances as described in the reference 17. If the changes of  $V_T$  and  $V_B$  ( $\Delta V_T$ , and  $\Delta V_B$ ) observed upon the sudden reduction of basolateral  $\text{Cl}^-$  concentration are assumed to arise from the changes of both electromotive forces ( $\Delta E_S$ , and  $\Delta E_B$ ), then  $\Delta V_T$  and  $\Delta V_B$  can be described by the following equations:

$$\Delta V_T = \frac{\Delta E_B \cdot R_S + \Delta E_S \cdot (R_A + R_B)}{R_A + R_B + R_S} \quad (2)$$

$$\Delta V_B = \frac{\Delta E_B \cdot (R_A + R_S) + \Delta E_S \cdot R_B}{R_A + R_B + R_S} \quad (3)$$

Here, we introduce the ratio of the changes in electromotive forces,  $\alpha = \Delta E_S / \Delta E_B$ . By using this parameter, and rearranging Eqs. 2 and 3, we have:

$$\Delta V_B = \Delta V_T \cdot \frac{R_A + R_B \cdot \alpha + R_S}{(R_A + R_B) \cdot \alpha + R_S} \quad (4)$$

By using Eq. 4, we can assess three particular cases of  $\text{Cl}^-$  transport: (a) If  $\text{Cl}^-$  transport takes place exclusively via a paracellular route, this means  $\Delta E_B = 0$  and  $\alpha = \infty$ . In this limiting condition,  $\Delta V_B$  approximates  $\Delta V_T \cdot R_B / (R_A + R_B)$ . Consequently,  $\Delta V_B$  never exceeds  $\Delta V_T$ . This is not the case in the present study, since the observed values of  $\Delta V_B$  and  $\Delta V_T$  were 49.1 and 33.4 mV, respectively. (b) If 50% of  $\text{Cl}^-$  transport is due to paracellular flow, then  $\alpha = 1$  and  $\Delta V_B = \Delta V_T$ . This is not the case in the present study either. However, we can set a minimal value for the transcellular component of  $\text{Cl}^-$  transport. (c) If  $\text{Cl}^-$  transport takes place exclusively via a transcellular route, this means  $\Delta E_S = 0$  and  $\alpha = 0$ , at this limiting condition, and  $\Delta V_T$  equals  $\Delta V_B \cdot R_S / (R_A + R_S)$  so that  $\Delta V_T$  is always smaller than  $\Delta V_B$ . This case is possible for TAL. Since the cellular cable analysis is not feasible in TAL at present, we cannot determine the exact value of each resistance. However, we can say that the transcellular component of  $\text{Cl}^-$  transport in TAL is in the range of 50–100%. In agreement with this conclusion, we have reported that glutaraldehyde, 4,4'-diisothiocyanostilbene-2,2'-disulfonic acid, phloretin, acid pH, and  $\text{Ca}^{2+}$  elimination decrease  $\text{Cl}^-$  flux by 56 (5), 76 (5), 76 (6), and 64% (7), respectively, with little or no change in  $\text{Na}^+$  flux. Thus the present study would provide definite evidence that the major fraction of  $\text{Cl}^-$  transport takes place via the transcellular route, which consists of large  $\text{Cl}^-$

conductances in both the luminal and the basolateral membrane that exist in series. Under physiological conditions, this transcellular  $\text{Cl}^-$  conductance could contribute to  $\text{Cl}^-$  transport across TAL. If the  $V_T$  is 0 mV and if there is no  $\text{Cl}^-$  gradient across the epithelium, net  $\text{Cl}^-$  flux would be zero. However, it has been reported that the concentration of luminal  $\text{Cl}^-$  in TAL is higher by 35–40 mmol/liter than that of adjacent vasa recta (19, 20). If the distribution of  $\text{Cl}^-$  is entirely in equilibrium with each membrane potential, imposing a concentration gradient (35–40 mmol/liter higher in the lumen) would provide a favorable driving force for lumen-to-blood  $\text{Cl}^-$  transport (1). In a previous paper (6), we have reported that acidification of ambient fluid inhibits  $\text{Cl}^-$  transport across the hamster TAL. On the basis of the observation that the selective intracellular acidification with *o*-phenylacetate also inhibited the  $\text{Cl}^-$  permeability, we suggested that the transcellular route of  $\text{Cl}^-$  transport is sensitive to pH. This view is supported by the present observation that the acidification of bathing fluid abolished the deflection of  $V_B$  upon sudden reduction of basolateral  $\text{Cl}^-$  concentration.

In conclusion, the TAL of hamster kidneys is highly permeable to  $\text{Cl}^-$ . A considerable portion of this  $\text{Cl}^-$  permeability is accounted for by  $\text{Cl}^-$  conductances in both the luminal and the basolateral cell membranes. Acidification of the bathing fluid inhibits the membrane  $\text{Cl}^-$  conductance at least in the basolateral membrane.

## Acknowledgments

We would like to express our thanks to Dr. J. Taniguchi for his valuable discussion and Mrs. Y. Ueshima for her secretarial assistance.

This work was supported in part by a grant from the Osaka Kidney Foundation (OKF 87-0011).

## References

1. Imai, M., J. Taniguchi, and K. Tabei. 1987. Function of thin loops of Henle. *Kidney Int.* 31:565–579.
2. Imai, M. 1977. Function of the thin ascending limb of Henle of rats and hamsters perfused in vitro. *Am. J. Physiol.* 232:F201–F209.
3. Imai, M., and J. P. Kokko. 1974. Sodium, chloride, urea, and water transport in the thin ascending limb of Henle. Generation of osmotic gradients by passive diffusion of solutes. *J. Clin. Invest.* 53:393–402.
4. Imai, M., and J. P. Kokko. 1976. Mechanism of sodium and chloride transport in the thin ascending limb of Henle. *J. Clin. Invest.* 58:1089–1097.
5. Kondo, Y., K. Yoshitomi, and M. Imai. 1987. Effect of anion transport inhibitors and ion substitution on  $\text{Cl}^-$  transport in the thin ascending limb of Henle's loop. *Am. J. Physiol.* 253:F1206–F1215.
6. Kondo, Y., K. Yoshitomi, and M. Imai. 1987. Effect of pH on  $\text{Cl}^-$  transport in the thin ascending limb of Henle's loop. *Am. J. Physiol.* 253:F1216–F1222.
7. Kondo, Y., K. Yoshitomi, and M. Imai. 1988. Effect of  $\text{Ca}^{2+}$  on  $\text{Cl}^-$  transport in the thin ascending limb of Henle's loop. *Am. J. Physiol.* 254:F232–F239.
8. Burg, M. B., J. Grantham, and J. Orloff. 1966. Preparation and study of fragments of single rabbit nephron. *Am. J. Physiol.* 210:1293–1298.
9. Yoshitomi, K., C. Koseki, J. Taniguchi, and M. Imai. 1987. Functional heterogeneity in the hamster medullary thick ascending limb of Henle's loop. *Pfluegers Arch. Eur. J. Physiol.* 408:600–608.
10. Kashgarian, M., D. Biemesderfer, M. Caplan, and B. Borbush

- III. 1985. Monoclonal antibody to Na, K-ATPase: immunocytochemical localization along nephron segments. *Kidney Int.* 28:899-913.
11. Garg, L. C., M. A. Knepper, and M. B. Burg. 1981. Mineral corticoid effects on Na-K-ATPase in individual nephron segments. *Am. J. Physiol.* 240:F536-F544.
12. Katz, A. I., A. Doucet, and F. Morel. 1979. Na-K-ATPase activity along the rabbit, rat, and mouse nephron. *Am. J. Physiol.* 237:F114-F120.
13. Barry, P. H., and J. M. Diamond. 1970. Junctional potentials, electrolyte standard potentials and other problems in interpreting electrical properties of membrane. *J. Membr. Biol.* 3:93-121.
14. Schwartz, M. M., and M. A. Veenkatachalam. 1974. Structural differences in thin limbs of Henle: physiological implications. *Kidney Int.* 6:193-208.
15. Barrett, J. M., W. Kriz, B. Kaissling, and C. de Rouffignac. 1978. The ultrastructure of the nephrons of desert rodent (*Psammomys obesus*) kidney. II. Thin limb of Henle of long-looped nephrons. *Am. J. Anat.* 151:499-514.
16. Bachman, S., and W. Kriz. 1982. Histotopography and ultrastructure of the thin limbs of the loop of Henle in the hamster. *Cell Tissue Res.* 225:111-127.
17. Boulpaep, E. L., and H. Sackin. 1979. Equivalent electrical circuit analysis and rheogenic pumps in epithelia. *Fed. Proc.* 38:2030-2036.
18. Frömter, E. 1986. The electrophysiological analysis of tubular transport. *Kidney Int.* 30:216-228.
19. Hogg, R. J., and J. P. Kokko. 1978. Comparison between the electrical potential profile and the chloride gradients in the thin limbs of Henle's loop in rats. *Kidney Int.* 14:428-436.
20. Gelbart, D. R., C. A. Battilana, J. Bhattacharya, F. B. Lacy, and R. L. Jamison. 1978. Transepithelial gradient and fractional delivery of chloride in the thin loop of Henle. *Am. J. Physiol.* 235:F192-F198.